Original article

Tatsuki Kurei, Rino Tsushima, Yoko Okahisa, Satoshi Nakaba, Ryo Funada and Yoshiki Horikawa*

Creation and structural evaluation of the three-dimensional cellulosic material "White-Colored Bamboo"

https://doi.org/10.1515/hf-2020-0030
Received January 28, 2020; accepted May 7, 2020; published online July 22, 2020

Abstract: This study reports a new cellulosic material that maintains the original three-dimensional structure of bamboo and is produced by optimization of chemical treatments. Bamboo blocks were prepared from the current year culms of moso bamboo (*Phyllostachys edulis*) and subjected to three chemical treatments alone or in combination. Based on the color changes and Fourier transform infrared spectra, the combination of alkaline treatment with alcoholysis followed by Wise method was found to be an optimal treatment method. This serial treatment caused the blocks to become completely white and removed non-cellulosic components such as hemicellulose and lignin from the cell walls of the parenchyma as well as those of vascular bundles. This sample was named as "White-Colored Bamboo." Extensive structural evaluations from anatomical- to nano- level were performed using X-ray computed tomography, X-ray diffraction, and transmission electron microscopy incorporated with the 2,2,6,6-tetramethylpiperidine-1-oxyl radical (TEMPO)-mediated oxidation technique. These multiple observations showed that the white-colored bamboo maintained its inherent hierarchical structure, thus encouraging to produce functional biomaterials.

Keywords: delignification; FTIR spectroscopy; hierarchical structure; microfibril orientation.

***Corresponding author: Yoshiki Horikawa**, Institute of Agriculture, Tokyo University of Agriculture and Technology, Fuchu, 183-8509, Japan, E-mail: horikaw@cc.tuat.ac.jp. https://orcid.org/0000-0003-0204-0455
Tatsuki Kurei, Rino Tsushima, Satoshi Nakaba and Ryo Funada: Institute of Agriculture, Tokyo University of Agriculture and Technology, Fuchu, 183-8509, Japan
Yoko Okahisa: Fiber Science and Engineering, Kyoto Institute of Technology, Kyoto, 606-8585, Japan

1 Introduction

Bamboo is a perennial grass with lignified tissues and is widely distributed across temperate and tropical regions. It consists of more than 90% cellulose, hemicellulose, and lignin like wood. Specifically, the percentages of each component are 40% cellulose, 31% hemicellulose, 21% lignin, 2% protein, 4% extractives, 1% starch, and 1% ash (Rabemanolontsoa and Saka 2013). Importantly, bamboo has flexibility as well as toughness and elasticity, which makes it distinct from wood. These characteristics are supported by its hierarchical structure from hollow culms to tissue that is mainly composed of vascular bundles and parenchyma cells to microstructures in the cell wall (Kiryu et al. 2016; Obataya et al. 2007; Okahisa et al. 2018). Therefore, bamboo has been applied since ancient times to make various products, from traditional crafts to daily supplies (Liese and Köhl 2015).

Recently, cellulose nanofiber made from bamboo has attracted attention for new applications (Abe and Yano 2010; Okahisa et al. 2011; Okahisa and Sakata 2019; Tsuboi et al. 2014). As cellulose has excellent mechanical properties and thermal stability, it can be used as a reinforcing fiber for biocomposites (Siró and Plackett 2010). However, the development of this material breaks down the hierarchical structure, and thus does not retain the superior characteristics of bamboo. Thus, a material that possesses the properties of both cellulose and bamboo has not been produced.

Given such background, this study focused on creating a cellulosic material by selectively removing the non-cellulosic components from bamboo while retaining the original structure. Three different treatments were examined to remove non-cellulose components from bamboo, and then tested the materials to determine their structural properties.

2 Materials and methods

2.1 Sample preparation

Current year culms of moso bamboo (*Phyllostachys edulis*) were taken from a plantation at the Fuchu campus of the Tokyo University of

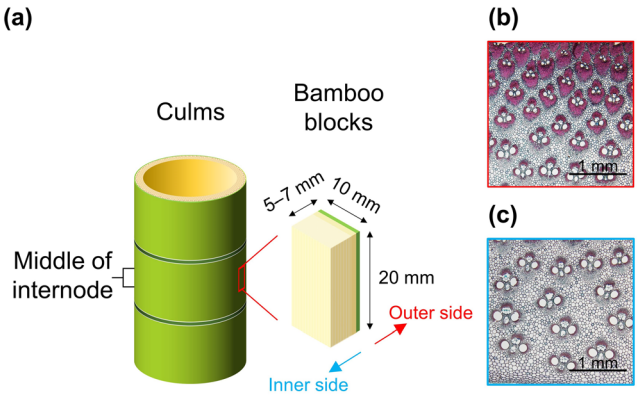

Figure 1: Sample structure (a), cross-section of outer side (b) and inner side (c) observed by light microscopy combined with safranin and Astra blue staining.

Agriculture and Technology. Bamboo blocks were obtained from the middle of the 9th internode. The size of blocks was 10 mm (tangential (T)) × 5–7 mm (radial (R)) × 20 mm (longitudinal (L)) (Figure 1a).

2.2 Chemical treatments for removing non-cellulosic components

Bamboo blocks were treated by conventional delignification methods; each method has a different mechanism, as shown in Table 1. Alkaline treatment (T_S) was carried out at 95 °C in 5% sodium hydroxide solution for 2 h. Alcoholysis (T_A) involved the following steps: (i) bamboo blocks were immersed in a solvent of propylene glycol:48.5% sulfuric acid = 99:1 based on a weight ratio, and (ii) soaked samples were placed in a portable reactor (TVS-N2, Taiatsu Techno, Tokyo, Japan) and heated at 150 °C for 1 h. The Wise method (T_W) is a bleaching treatment carried out by using sodium chlorite solution with acetic acid (Wise et al. 1946). The samples were soaked in bleaching solution for more than 7 h at 75 °C with the addition of these reagents after every hour until the color of the samples was no longer changed. The obtained bamboo blocks were freeze-dried for following different analyzes.

2.3 FTIR spectroscopy

Bamboo blocks before and after the chemical treatments were cut from the outer and inner sides because the treatment progress was predicted to vary depending on the distribution of vascular bundles and parenchyma cells in the radial direction (Figure 1b, c). The chemical components of these specimens were measured by attenuated total reflection accessory with Fourier transform infrared (FTIR) spectroscopy (Spectrum Frontier, PerkinElmer, Waltham, MA, USA). The spectra were recorded from the range of 2000–500 cm^{-1} at a resolution of 4 cm^{-1} with an acquisition of eight scans for each specimen. After applying the ATR corrected function using the accompanying software package followed by baseline correction, the spectra were normalized based on the band at 1030 cm^{-1} in the fingerprint region, whose absorbance was taken to be 1. Non-cellulosic components were evaluated from bands at 1730 cm^{-1} and approximately 1510 cm^{-1} which corresponded to hemicellulose (C=O stretching vibration in the acetyl group and carboxylic acid) and lignin (aromatic skeletal vibration), respectively (Faix 1991; Horikawa et al. 2019).

Table 1: Abbreviated names of different chemical treatments applied in this study.

Abbreviated name	Procedure
T_S	Boiling with 5% sodium hydroxide solution
T_A	Alcoholysis
T_W	Wise method
$T_{A\text{-}S}$	$T_A \rightarrow T_S$
$T_{A\text{-}W}$	$T_A \rightarrow T_W$
$T_{S\text{-}A}$	$T_S \rightarrow T_A$
$T_{S\text{-}W}$	$T_S \rightarrow T_W$
$T_{S\text{-}A\text{-}W}$	$T_S \rightarrow T_A \rightarrow T_W$

2.4 X-ray computed tomography

Dried bamboo blocks were scanned at 32 kV and 470 µA using X-ray computed tomography (X-ray CT; SkyScan 2211, Bruker, Billerica, MA, USA) to create 2D- and 3D-reconstructed images. A rotation step of 0.4 degrees and resolution of 10 µm was used. Additionally, vascular bundles of bamboo blocks were visualized by image processing.

2.5 X-ray diffraction analysis

X-ray fiber diffraction diagrams of the outer and inner specimens were obtained using a wide-angle X-ray diffractometer (R-AXIS RAPID, Rigaku, Tokyo, Japan) at a voltage of 32 kV and current of 250 mA to investigate the microfibril orientation. For these measurements, the longitudinal direction of the specimens was set along the vertical direction of the imaging plate, and the X-ray was perpendicularly irradiated to the tangential face of the bamboo block. The microfibril angles were calculated from the 200-plane reflection of cellulose I_β by Gaussian function fitting.

X-ray diffractograms were also obtained in reflection mode by employing an automated multipurpose X-ray diffractometer (SmartLab, Rigaku, Tokyo, Japan) at a voltage of 50 kV and current of 250 mA.

2.6 Transmission electron microscopy

After chemical treatments, a specimen was suspended in water and oxidized using the 2,2,6,6-tetramethylpiperidine-1-oxyl radical (TEMPO)/NaBr/NaClO system (Saito et al. 2006). This reaction was conducted at pH 10 and room temperature for 2 h. Next, the oxidation product was reduced by adding $NaBH_4$ and stirring for 3 h (Takaichi et al. 2014). After repeated washing and subsequent homogenization with a double-cylinder-type homogenizer (Hiscotron, Microtec, Chiba, Japan), individual bamboo cellulose microfibrils, dispersed in water, were obtained.

The TEMPO-oxidized cellulose suspension was spotted onto a copper grid supported by a carbon film (ELS-C10, Okenshoji, Tokyo, Japan). Cellulose microfibrils were observed by negative staining with 2% uranyl acetate using transmission electron microscopy (TEM; JEM-1400 Plus, JEOL, Tokyo, Japan) at 80 kV.

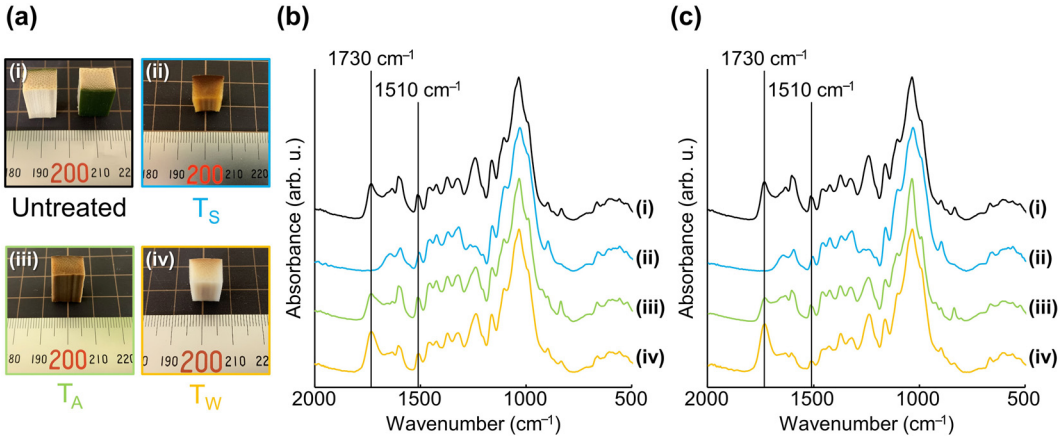

Figure 2: Sample images (a) and fourier transform infrared (FTIR) spectra of bamboo specimens from outer side (b) and inner side (c) in each single treatment: (i) untreated, (ii) T_S, (iii) T_A, and (iv) T_W.

3 Results and discussion

3.1 Determination of optimal treatments for removing non-cellulosic components

After T_S and T_A, the color of the bamboo blocks became darker (Figure 2a), which may have resulted from the production of colored components by excessive decomposition of hemicellulose or modification of lignin. T_W also changed the color of the samples to brown on the outer side due to oxidation. FTIR spectra after each single treatment showed bands at 1730 cm^{-1} (assigned to hemicellulose) or 1510 cm^{-1} (assigned to lignin) or both decrease on the outer and inner sides (Figure 2b, c). However, each treatment alone could not completely remove the non-cellulosic components.

In the case of $T_{A\text{-}S}$ and $T_{S\text{-}A}$, the colors of the bamboo blocks were similar to those of the samples after T_S and T_A (Figure 3a), where the band at 1510 cm^{-1} remained (Figure 3b, c). After $T_{A\text{-}W}$ the band at 1510 cm^{-1} disappeared in the spectrum from the inner side with the progression of decolorization, whereas the outer side was not significantly changed compared to the untreated control (Figure 2b). For $T_{S\text{-}W}$, although the outer side remained colored, the bands at 1730 and 1510 cm^{-1} disappeared. This indicates that the amounts of lignin and hemicellulose were below the FTIR detection limit. Therefore, both combinations of the 2 treatments were not completely effective.

Finally, when $T_{S\text{-}A\text{-}W}$ was conducted on the bamboo blocks, even the outer sides were completely whitened (Figure 4a, b). Furthermore, the FTIR spectra after $T_{S\text{-}A\text{-}W}$ did not show bands at 1730 or 1510 cm^{-1} on either side. The FTIR spectra after $T_{S\text{-}A\text{-}W}$ exhibited spectra similar to that of cellulose purified from bamboo powder (Figure 4c) using a conventional method for lignified samples (Horikawa 2017). As a result, $T_{S\text{-}A\text{-}W}$ was determined to be the optimal technique for selectively removing non-cellulosic

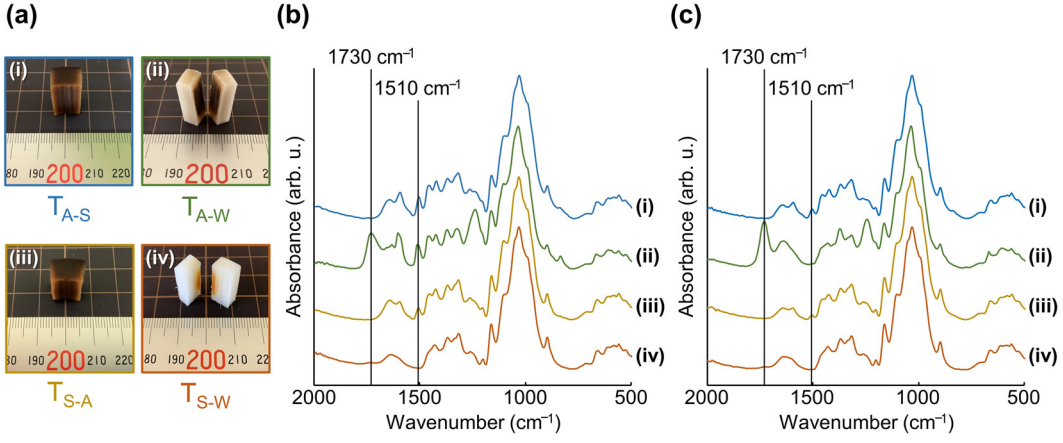

Figure 3: Sample images (a) and FTIR spectra of bamboo specimens from outer side (b) and inner side (c) when two treatments were combined: (i) $T_{A\text{-}S}$, (ii) $T_{A\text{-}W}$, (iii) $T_{S\text{-}A}$, and (iv) $T_{S\text{-}W}$. (ii), (iv) show longitudinal planes.

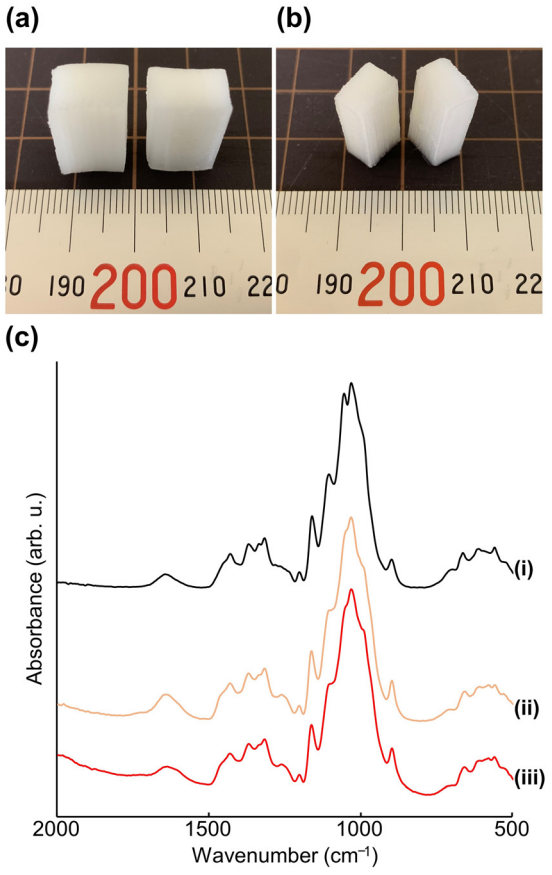

Figure 4: Sample images of front and back sides (a), longitudinal plane (b) and FTIR spectra (c) of purified cellulose from bamboo powder (i) and obtained from specimens (ii, iii). (ii) was from the outer side and (iii) was from the inner side.

components from bamboo blocks. Li et al. (2016) conducted sodium chlorite treatment alone and successfully developed delignified wood from Balsa, which is a low-density wood material. In contrast, bamboo is a higher-density material that cannot undergo complete delignification and decolorization using sodium chlorite alone (Figure 2). However, combining the three processes resulted in complete delignification and decolorization (Figure 4). In this study, the bamboo block after $T_{S\text{-}A\text{-}W}$ was named as "White-Colored Bamboo", and its hierarchical structure was further investigated.

3.2 Evaluation of hierarchical structure

3.2.1 Anatomical structure

The anatomical structures of untreated and white-colored bamboo were compared using X-ray CT (Figure 5). Although cracks and shrinkage caused by drying were observed, white-colored bamboo did not significantly change the shape and distribution of vascular bundles (Figure 5a, d). In addition, the 3D morphology (Figure 5b, e) and arrangement of vascular bundles (Figure 5c, f) were also unchanged. As a consequence, the parenchyma cells appeared to retain their original form.

Some particles were observed in the inner side of the untreated bamboo (Figure 5c) and in white-colored bamboo (Figure 5f). It has been reported that starch grains are most

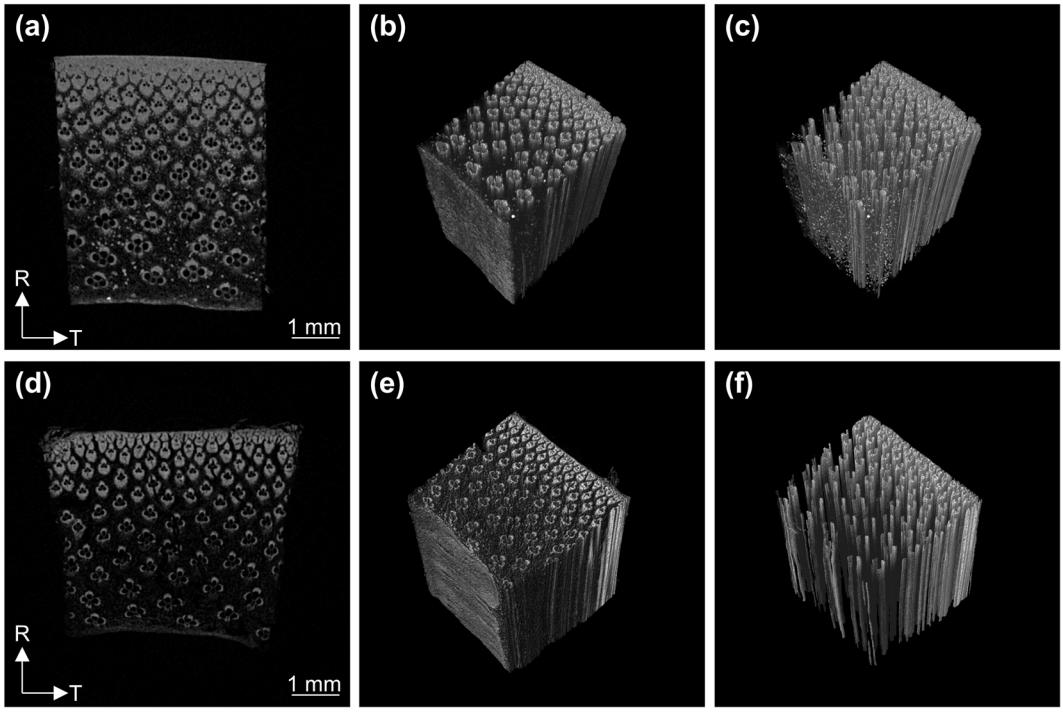

Figure 5: Cross-sections (a), (d) and 3D-reconstruction images (b), (c), (e), and (f) of bamboo blocks scanned by X-ray CT. (a–c) shows untreated bamboo while (d–f) are white-colored bamboo (after $T_{S\text{-}A\text{-}W}$). (c) and (f) are modified from (b) and (d) to visualize vascular bundles by image processing. The length in L and T directions differs from the actual sample size because of the measurement range.

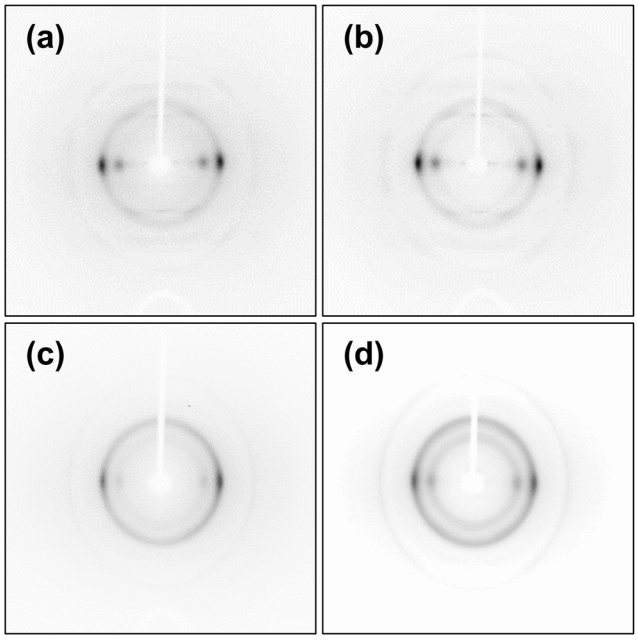

Figure 6: X-ray fiber diffraction diagrams from the outer side (a, b) and inner side (c, d). (a, c) were obtained from untreated while (b, d) were acquired from white-colored bamboo blocks.

abundant on the inner side and decrease towards the outer side (Okahisa et al. 2007). Therefore, these particles may have been starch grains, suggesting that their quantity was reduced by the chemical treatments.

3.2.2 Orientation and crystalline structure of cellulose microfibrils

Figure 6 shows the X-ray fiber diffraction diagrams of the inner and outer sides of the specimens. The diffraction patterns differed between the outer (Figure 6a, b) and inner sides (Figure 6c, d) because of differences in the ratio of fiber and parenchyma cells in the radial direction, as previously reported by Okahisa et al. (2018). This trend on both sides was maintained before and after the treatments; thus, from a qualitative perspective, the microfibril orientation was undisturbed.

Table 2: Microfibril angles of bamboo blocks calculated from the 200-plane reflection in Figure 6.

	Microfibril angles (deg.)	
	Outer side of vascular bundles	Inner side of vascular bundles
Untreated bamboo	2.2	4.0
White-colored bamboo	1.9	3.4

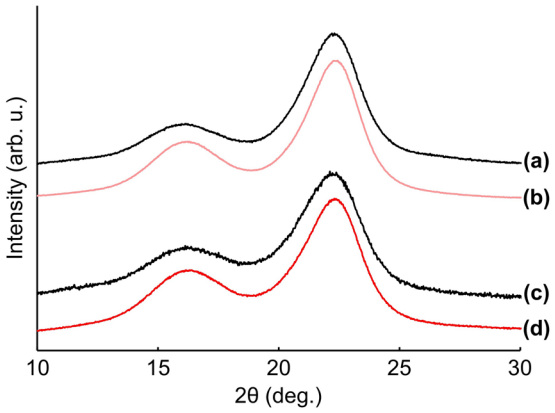

Figure 7: X-ray diffractograms from outer side (a, b) and inner side (c, d). (a, c) obtained from untreated, whereas (b, d) were acquired from white-colored bamboo blocks.

For more quantitative assessment, the microfibril angles were calculated from a fiber diffraction diagram obtained using 200-plane reflection. The microfibril angles of untreated bamboo were 2.2 and 4.0 degrees on the outer and inner sides, respectively (Table 2). The cell wall layer of fiber or parenchyma cell layer has a polylamellar structure (Liese and Köhl 2015). Particularly, the fiber cell wall structure has alternating thick and thin layers. Microfibrils in the former layer are orientated nearly parallel to the cell axis, whereas microfibrils in the latter layer are oriented nearly perpendicular to the cell axis (Parameswaran and Liese 1976). Lower microfibril angles on the outer side which contains densely packed with fibers are formed because of the longitudinal orientation of the thick layers. After the treatments, the microfibril angles were 1.9 and 3.4 degrees on the outer and inner sides, respectively (Table 2), showing similar tendencies to form fibers which were close to those of untreated bamboo. Hence, the microfibril orientation in the cell wall was maintained in the white-colored bamboo.

X-ray diffraction analysis also revealed the crystalline structure of cellulose in the cell wall layer (Figure 7). Before and after treatment, bamboo specimens with the outer (Figure 7a, b) and the inner (Figure 7c, d) sides showed a typical diffraction pattern of cellulose I (Wada et al. 1997). The obvious sharpening of the diffraction peaks in the white-colored bamboo resulted from the removal of matrix components which led to a better microfibril orientation. Consequently, the chemical treatments used in this experiment did not cause crystalline modification.

3.3 Morphology of cellulose microfibrils

The TEM imaging results confirmed that the TEMPO-oxidized cellulose microfibrils obtained from white-colored bamboo

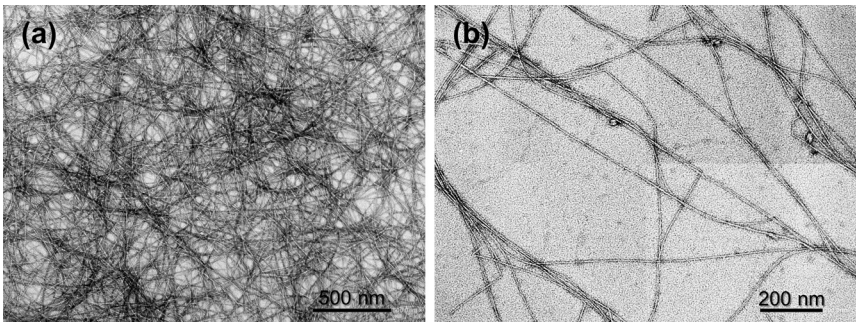

Figure 8: Transmission electron microscopy (TEM) images of 2,2,6,6-tetramethylpiperidine-1-oxyl radical (TEMPO)-oxidized cellulose microfibrils obtained from white-colored bamboo: (a) overview and (b) magnified view.

were uniformly individualized (Figure 8a). The microfibril width calculated from the magnified view was 3.77 ± 0.95 nm (Figure 8b). The width of approximately 3–4 nm is similar to that of terrestrial plants (Kuramae et al. 2014). In addition, cellulose microfibrils were much longer and not fragmented. Cellulose microfibrils obtained from terrestrial plants become fragmented to approximately 150 nm by acid hydrolysis (Horikawa et al. 2018; Nickerson and Habrle 1947; Nishiyama et al. 2003). Harsh alkaline treatments also decrease the length of microfibrils (Pavasars et al. 2003). However, these phenomena were not observed for white-colored bamboo. Thus, the morphology of cellulose microfibrils was preserved after treatment.

4 Conclusions

This study demonstrated the successful creation of the "White-Colored Bamboo" in which non-cellulose components were selectively removed from the bamboo block. FTIR spectroscopy clarified that the optimal chemical treatment was $T_{S\text{-}A\text{-}W}$: boiling in 5% sodium hydroxide solution → alcoholysis → Wise method. Multiple evaluations using X-ray CT, X-ray diffraction, and TEM revealed that the original macro- to micro- structure was maintained. In conclusion, "White-Colored Bamboo" was successfully characterized as a novel biomaterial with the structure of bamboo despite being a cellulosic material. Thus, it is possible to expand the utilization of bamboo to develop sustainable products. Further studies are needed to compare the material characteristics of white-colored bamboo to those of conventional cellulosic materials.

Acknowledgments: The authors would like to thank Mr. Watanabe N. of Tokyo University of Agriculture and Technology for providing the bamboo samples. The authors appreciate Dr. Noguchi K. of Tokyo University of Agriculture and Technology for the X-ray diffraction analysis and Mr. Sano H. of Tokyo Metropolitan Industrial Technology Research for the X-ray CT experiment.

Author contribution: All the authors have accepted responsibility for the entire content of this submitted manuscript and approved submission.

Research funding: This research study was jointly supported by Grants-in-Aid for Scientific Research (KAKENHI) [Grant number 19K06167] from the Japan Society for the Promotion of Science (JSPS). This work was also supported by Grants-in-Aid for Sugiyama Chemical & Industrial Laboratory.

Conflict of interest statement: The authors declare that they have no conflict of interest.

References

Abe, K. and Yano, H. (2010). Comparison of the characteristics of cellulose microfibril aggregates isolated from fiber and parenchyma cells of Moso bamboo (*Phyllostachys pubescens*). Cellulose 17: 271–277.

Faix, O. (1991). Classification of lignins from different botanical origins by FT-IR spectroscopy. Holzforschung 45: 21–27.

Horikawa, Y., Shimizu, M., Saito, T., Isogai, A., Imai, T., and Sugiyama, J. (2018). Influence of drying of chara cellulose on length/length distribution of microfibrils after acid hydrolysis. Int. J. Biol. Macromol. 109: 569–575.

Horikawa, Y., Hirano S., Mihashi, A., Kobayashi, Y., Zhai, S., and Sugiyama, J. (2019). Prediction of lignin contents from infrared spectroscopy: chemical digestion and lignin/biomass ratios of *Cryptomeria japonica*. Appl. Biochem. Biotechnol. 188: 1066–1076.

Horikawa, Y. (2017). Assessment of cellulose structural variety from different origins using near infrared spectroscopy. Cellulose 24: 5313–5325.

Kiryu, T., Miyoshi, Y., and Furuta, Y. (2016). The mechanism of improvement of physical properties of moso bamboo (*Phyllostachys pubescens*) with increasing age I. Mokuzai Gakkaishi 62: 61–66.

Kuramae, R., Saito, T., and Isogai, A. (2014). TEMPO-oxidized cellulose nanofibrils prepared from various plant holocelluloses. React. Funct. Polym. 85: 126–133.

Li, Y., Fu, Q., Yu, S., Yan, M., and Berglund, L. (2016). Optically transparent wood from a nanoporous cellulosic template: combining functional and structural performance. Biomacromolecules 17: 1358–1364.

Liese, W. and Köhl, M. (2015). *Bamboo: The plant and its uses*. Springer, New York.

Nickerson, R.F. and Habrle, J.A. (1947). Cellulose intercrystalline structure. Ind. Eng. Chem. 39: 1507–1512.

Nishiyama, Y., Kim, U.J., Kim, D.Y., Katsumata, K.S., May, R.P., and Langan, P. (2003). Periodic disorder along ramie cellulose microfibrils. Biomacromolecules 4: 1013–1017.

Obataya, E., Kitin, P., and Yamauchi, H. (2007). Bending characteristics of bamboo (*Phyllostachys pubescens*) with respect to its fiber-foam composite structure. Wood Sci. Technol. 41: 385–400.

Okahisa, Y. and Sakata, H. (2019). Effects of growth stage of bamboo on the production of cellulose nanofibers. Fibers Polym. 20: 1641–1648.

Okahisa, Y., Yoshimura, T., Sugiyama, J., Horikawa, E.Y., and Imamura, Y. (2007). Longitudinal and radial distribution of free glucose and starch in moso bamboo (*Phyllostachys pubescens* Mazel). J. Bamboo Rattan 6: 21–31.

Okahisa, Y., Abe, K., Nogi, M., Nakagaito, A.N., Nakatani, T., and Yano, H. (2011). Effects of delignification in the production of plant-based cellulose nanofibers for optically transparent nanocomposites. Compos. Sci. Technol. 71: 1342–1347.

Okahisa, Y., Kojiro, K., Kiryu, T., Oki, T., Furuta, Y., and Hongo, C. (2018). Nanostructural changes in bamboo cell walls with aging and their possible effects on mechanical properties. J. Mater. Sci. 53: 3972–3980.

Parameswaran, N. and Liese, W. (1976). On the fine structure of bamboo fibres. Wood Sci. Technol. 10: 231–246.

Pavasars, I., Hagberg, J., Borén, H., and Allard, B. (2003). Alkaline degradation of cellulose: mechanisms and kinetics. J. Polym. Environ. 11: 39–47.

Rabemanolontsoa, H. and Saka, S. (2013). Comparative study on chemical composition of various biomass species. RSC Adv. 3: 3946–3956.

Saito, T., Nishiyama, Y., Putaux, J.L., Vignon, M., and Isogai, A. (2006). Homogeneous suspensions of individualized microfibrils from TEMPO-catalyzed oxidation of native cellulose. Biomacromolecules 7: 1687–1691.

Siró, I. and Plackett, D. (2010). Microfibrillated cellulose and new nanocomposite materials: a review. Cellulose 17: 459–494.

Takaichi, S., Saito, T., Tanaka, R., and Isogai, A. (2014). Improvement of nanodispersibility of oven-dried TEMPO-oxidized celluloses in water. Cellulose 21: 4093–4103.

Tsuboi, K., Yokota, S., and Kondo, T. (2014). Difference between bamboo- and wood-derived cellulose nanofibers prepared by the aqueous counter collision method. Nord Pulp Paper Res. J. 29: 69–76.

Wada, M., Okano, T., and Sugiyama, J. (1997). Synchrotron-radiated X-ray and neutron diffraction study of native cellulose. Cellulose 4: 221–232.

Wise, L.E., Murphy, M., and D'Addieco, A.A. (1946). Chlorite holocellulose, its fractionation and bearing on summative wood analysis and on studies on the hemicelluloses. Pap. Trade J. 122: 35–43.